Title

THERMAL PROCESSING OF FERRITIC 5MN STEEL FOR TOUGHNESS AT CRYOGENIC TEMPERATURES

Author

Niikura, K.

Publication Date

1979-11-01

LBL-9798
Preprint

Lawrence Berkeley Laboratory
UNIVERSITY OF CALIFORNIA

Materials & Molecular Research Division

Submitted to Metallurgical Transactions

THERMAL PROCESSING OF FERRITIC 5MN STEEL FOR TOUGHNESS AT CRYOGENIC TEMPERATURES

K. Niikura and J.W. Morris, Jr.

November 1979

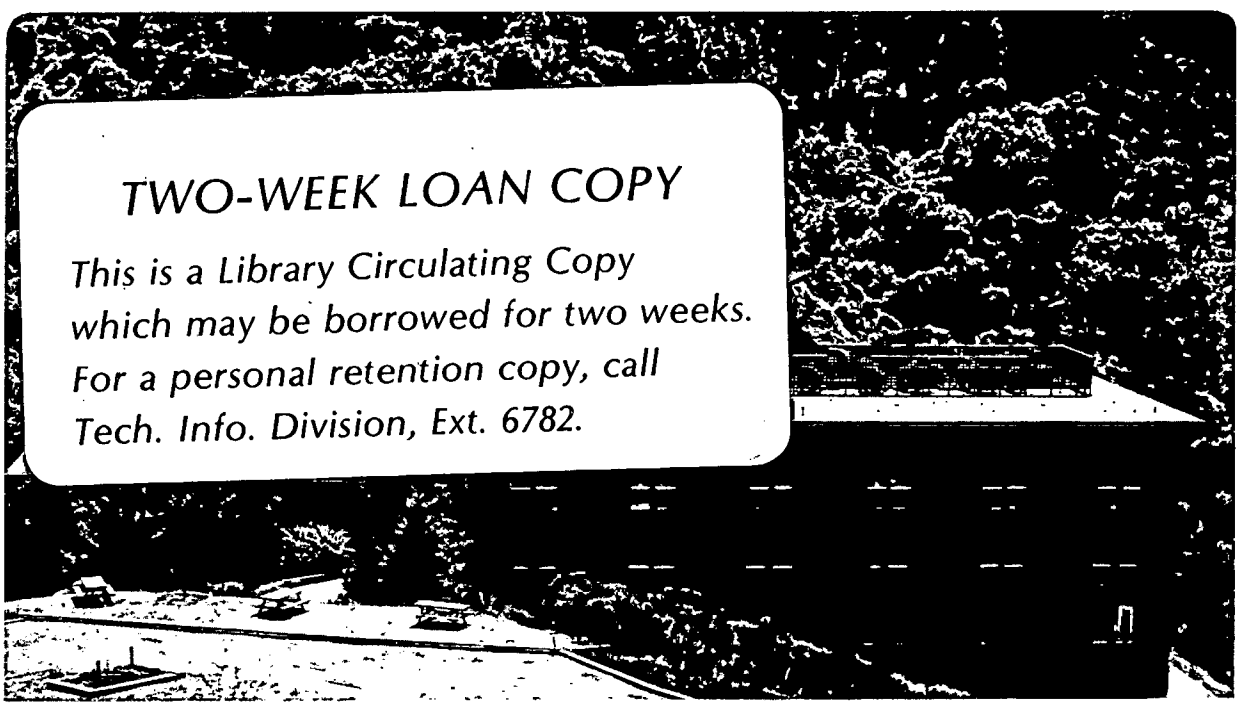

Prepared for the U.S. Department of Energy under Contract W-7405-ENG-48

DISCLAIMER

THERMAL PROCESSING OF FERRITIC 5MN STEEL FOR TOUGHNESS AT CRYOGENIC TEMPERATURES

By

M. Niikura* and J. W. Morris, Jr.

Department of Materials Science and Mineral Engineering and
Materials and Molecular Research Division, Lawrence Berkeley Laboratory,
University of California, Berkeley, California 94720.

*Present address: Central Research Laboratories,
Nippon Kokan K.K., Tokoyo, Japan.

ABSTRACT

It is shown that a thermal treatment which combines grain refinement with an intercritical temper (the 2BT treatment) may be used to achieve an excellent combination of strength and toughness in a nickel-free ferritic steel of nominal composition Fe-5Mn-0.2Mo-0.04C at temperatures as low as -196°C. The properties achieved are attributed to a symbiotic influence between the grain refinement treatment and the introduction of thermally stable retained austenite during intercritical tempering, a conclusion supported by a comparison of the results to those obtained with simpler heat treatments. The influence of carbon, manganese, and nickel additions to the base compositions are studied. An increase in carbon content above 0.04 wt.% causes a deterioration in toughness, as does an increase in manganese to 8 wt.%. An addition of 1-3 wt.% nickel is beneficial giving an increase in alloy strength at -196°C without loss of toughness.

I. INTRODUCTION

The steels commonly specified for structural applications at LNG and lower temperatures, 9%Ni steel, austenitic stainless steels, and Invar alloys, all have a relatively high nickel content. While the nickel addition contributes significantly to the good low-temperature properties of these alloys, it also adds substantially to the cost. Consequently, there is an incentive to develop alloys which retain good or cryogenic properties with reduced nickel content. Steels containing 5 to 6% nickel were recently introduced in the United States[1] and in Japan[2] in response to this need. Further decreases in the nickel content would be desirable.

Of the common alloying elements in steel, manganese is the most obviously attractive as a substitute for nickel in cryogenic alloys. Manganese is readily available, relatively inexpensive, and has an intriguing metallurgical similarity to nickel in its effect on the microstructures and phase relationships of iron-base alloys. Research on the cryogenic properties of Fe-Mn alloys has hence been undertaken in a number of laboratories[3-8]. While this research has yielded several alloys which retain excellent toughness at cryogenic temperatures, the alloys are austenitic grades which are relatively low in structural strength and very high in manganese content (18-25% by weight).

In contrast to the Fe-Ni cryogenic steels, whose metallurgy and cryogenic mechanical properties have been extensively investigated, until very recently there had been relatively little research on the low temperature mechanical properties of ferritic Fe-Mn steels. The published work[8-10] was largely discouraging. The ferritic Fe-Mn grades were found to have

high transition temperatures and to be particularly liable to intergranular fracture, either because of a sensitivity to temper embrittlement, in the low Mn grades, or because of an apparently inherent bias toward intergranular failure at higher Mn contents.

Despite the discouraging results of earlier research, the metallurgical similarity of Mn and Ni in ferritic steels seemed sufficient to warrant a program of research into the cryogenic potential of ferritic Fe-Mn steels, which was begun in this laboratory several years ago. This program took two rather different technical paths, which addressed the two distinct types of ferritic alloys which may be based on the Fe-Mn binary[3,11], illustrated in Figs. 1 and 2. When the manganese concentration is relatively low (4-10 wt%), an Fe-Mn binary alloy will transform on quenching to α' (BCC) martensite with a dislocated lath substructure (Fig. 2a) strongly resembling that of Fe-Ni alloys of similar alloy content. With higher manganese additions ($\approx$10-14 wt.%), however, a competing transformation of the parent austenite to the hexagonal, ε-martensite phase intrudes. The substructure of the alloy changes substantially, and consists of block islands of dislocated α' martensite divided by regions which contain ε-martensite (Fig. 2b) and retained austenite in a volume fraction which increases with the Mn content. The low Mn martensites have relatively high ductile-brittle transition temperatures in the as-quenched condition. Their transition temperatures are determined by a shift in fracture mode from ductile rupture to transgranular quasi-cleavage (Fig. 2c). The high Mn martensites also have relatively high ductile-brittle transition temperatures but, in this case, the associated change in fracture mode is to a catastrophic intergranular fracture (Fig. 2d).

Research on the ferritic Fe-Ni steels has shown that there are at least two microstructural modifications which lead to a decrease in the ductile-brittle transition temperature[12]: grain refinement[13-15], and the introduction of a slight admixture of thermally stable austenite through an intercritical tempering treatment (i.e., a heat treatment at a relatively low temperature in the two-phase ($\alpha+\gamma$) region)[16-18]. Both these microstructural modifications may be accomplished through thermal treatments which are suitable for the processing of steel plate. In the case of Fe-Mn alloys with high manganese contents ($\geq$ 10 wt.%) the conventional thermal treatments cannot be effectively used because of modifications in phase transformation behavior caused by the intrusion of the ε-martensite phase[11]. An alternate approach, which involves the addition of boron to directly suppress the tendency toward intergranular fracture, has recently been successfully employed to achieve good cryogenic toughness in Fe-12Mn steels[19]. Fe-Mn alloys of lower manganese content should, however, be amenable to processing by the conventional Fe-Ni thermal treatments.

In earlier work in this laboratory[11] an attempt was made to toughen an Fe-8Mn-0.2Ti alloy for cryogenic use by combining a cyclic thermal treatment, to achieve an ultrafine grain size, with a final intercritical temper to impart a distribution of retained austenite. The treatment employed has previously been designated the "2BT" treatment[12,15] and has been shown capable of suppressing the ductile-brittle transition temperature of commercial 9Ni steel to below 4°K(-269°C). However, while a substantial decrease in the ductile brittle transition temperature was achieved, the transition temperature remained above liquid nitrogen temperature (-196°C) with the consequence that the alloy is not suitable for cryogenic structural use. An analysis of the results revealed

the intrusion of ε-martensite during the final tempering treatment[11], which may have reduced the efficiency of this treatment in lowering the transition temperature.

In parallel work, Niikura and coworkers[20] showed that it is possible to introduce a significant fraction of thermally stable austenite into Fe-5Mn alloys containing a small carbon addition through a suitable intercritical temper. No evidence of ε-phase intrusion was found. A similar result was obtained by Miller[21] in research on 4Mn steels. Since the difficulties encountered in the Fe-8Mn alloy seemed to arise from the intrusion of the ε-phase during the final tempering treatment, it was decided to explore the cryogenic potential of 2BT-treated Fe-Mn alloys of lower manganese content. As shown in the following, these can be designed and processed to have excellent cryogenic structural properties.

II. EXPERIMENTAL PROCEDURE

Eight 10kg ingots were prepared by induction melting under an argon gas atmosphere. The compositions of these ingots are given in Table I. Ingots A and B are essentially identical in nominal composition which is, in weight percent, Fe-5Mn-0.2Mo-0.04C. These steels contained intentional additions of carbon (0.04%), as in commercial Fe-Ni steels, and Mo (0.2%) to enhance resitance to temper embrittlement. Ingots C, D, and E were cast to determine the effect of higher additions of carbon to the base composition. Ingots F and G were cast to assess the effect of a small addition of nickel. Ingot H was cast to determine the effect of a higher manganese content and differs from the base composition in having approximately 8 wt.% Mn. This ingot also proved to have a slightly higher

carbon content, 0.065 wt.%, than is present in the base composition.

The ingots were homogenized in vacuum at 1200°c for 24 hours, and then upset cross-forged at 1100°C to 12.7mm (0.5 in.) thick or 25.4mm (1.0 in.) thick plates. The plates were annealed at 1100°C for two hours under argon gas to remove prior deformation strain and air-cooled.

To impart cryogenic toughness, the alloys were given an appropriate modification of the "2BT" treatment diagrammed in Fig. 3. The treatment consists of a four-step thermal cycling to refine the alloy grain size, followed by a final intercritical temper to introduce a distribution of thermally stable retained austenite. The grain refinement treatment consists of an austenite reversion (Step 1A), followed by an intercritical anneal (Step 1B), followed by a repetition of these (Steps 2A and 2B). The temperatures used in this cycling treatment were chosen from the results of dilatometric studies[13]. The 1A and 2A temperatures were selected to lie slightly above the temperature (A_f) at which the reversion reaction to the austenite phase is believed to occur, primarily through a reverse shear transformation. The intercritical annealing temperature, used in steps 1B and 2B, was chosen to lie somewhat below the A_f temperature. In these heat treatment steps the intent is to obtain a partial reversion to austenite which proceeds through a nucleation and growth mechanism. After grain refinement the alloys were given an intercritical temper to introduce a distribution of thermally stable retained austenite. The alloys were water-quenched after each heat treatment.

The temperatures employed in the heat treatment are tabulated in Table II. It was not found necessary to adjust heat treatment temperatures for small changes in carbon content, but the addition of Ni or Mn

to the base composition did require a modification of the temperatures used in the "2BT" grain refinement treatment.

To study the effect of heat treatment on cryogenic properties, two alternate heat treatments were used. The first was a standard quench and temper (QT) treatment, similar to that often employed in the processing of 9Ni steel for cryogenic use, in which the alloys were water-quenched after initial austenization and given an intercritical temper to introduce retained austenite. The second treatment was a three-step heat treatment, designated QQ'T, which resembles that used in the commercial processing of 5-6% nickel cryogenic steels[1,2]. In the QQ'T processing the alloys were given the 1A and 1B treatments indicated in Table II and were then intercritically tempered.

Since the heat-treated specimens were small samples, all heat treatments were conducted either in inert atmosphere or after sealing in stainless steel bags.

Following heat treatment, the mechanical properties of the alloys were determined at room temperature and at cryogenic temperature through a combination of tensile, impact, and fracture toughness tests. The tensile properties of the alloy were measured using subsized, round tensile specimens of 12.7mm (0.5 in.) gauge length and 3mm (0.1 in.) gauge diameter tested at a cross-head speed of 0.08 cm/min (0.03 in/min). The impact toughness of the alloys was measured using Charpy V-notched specimens machined and tested according to ASTM standards. The fracture toughness was measured with compact tension specimens of 17.8mm (0.7 in.) thickness, 50.8mm (2.0 in.) width, and 25.4mm (1.0 in.) initial crack length. The tests were conducted at -196°C in a MTS machine equipped

with a liquid nitrogen cryostat. Since the thickness of these specimens did not meet ASTM requirements for plane strain conditions, the fracture toughness (K_{1c}) values were estimated from equations based on the "equivalent energy"[22] and "J-integral"[23] concepts.

Microstructural and fractographic analyses were conducted using standard optical, transmission electron microscopic, and scanning electron microscopic techniques. The retained austenite content in the heat-treated samples was measured by conventional x-ray diffraction, comparing the integrated intensities of the $(200)_\alpha$ and $(200)_\gamma$ peaks.

III. RESULTS AND DISCUSSION

A. Microstructural Response to Heat Treatment.

The microstructures obtained after the three heat treatments, QT, QQ'T, and 2BT, are illustrated by the optical micrographs presented in Fig. 4. All three microstructures consist primarily of tempered martensite. It is, however, evident that the 2BT material has been microstructurally refined relative to the material produced by the other treatments. The martensite packet size, which is the effective grain size in the lath martensite structure[18], is 3-8μm in the 2BT material as compared to 10-20μm in the QT and QQ'T alloys. The microstructural refinement accomplished by the 2BT treatment and the final microstructure obtained strongly resembles those in ferritic Fe-Ni alloys processed in a similar way[14,15].

Transmission electron microscopic studies of the microstructure of the 2BT material are presented in Figs. 5 and 6. Figure 5 shows the evolution of the microstructure of the 2BT material as a function of tempering time. Figure 6 shows the retention of precipitated austenite

in the 2BT material after 4 hours intercritical tempering.

These transmission electron microscopic studies illustrate the two characteristic microstructural changes associated with intercritical tempering[24]: the recovery of transformation-inducted dislocations into an equiaxed subgrain structure, and the formation and retention of particles of austenite phase along the martensite lath boundaries. Figure 5 shows the equiaxed, submicron sized subgrains which develop inside martensite packets after 4 hours tempering. The subgrains are well recovered and contain very low densities of internal dislocations. The subgrains are presumably formed from the dense distribution of transformation-induced defects which are present in the 2B starting material, as illustrated in Fig. 5a. The austenite retained in the 2BT structure after cooling to room temperature is apparent in the diffraction pattern presented in Fig. 6, and its morphology and location in the microstructure is revealed in the accompanying dark-field transmission electron micrograph. As in the case of iron-nickel ferritic alloys, the austenite appears to form along lath boundaries of the parent martensite and has a Kurdjumov-Sachs relation to the parent martensite. There is a strong tendency for only a single variant of the austenite to form within a given packet.

The volume fraction of retained austenite present after tempering and cooling to room temperature was determined as a function of tempering time for the three heat treatments. The x-ray diffraction results are presented in Fig. 7. The 2BT material contains 8 volume percent retained austenite after tempering for 4 hours, and 12 percent retained austenite after tempering for 16 hours. The QQ'T material develops a similar retained austenite content, although there is an apparent tendency for the austenite volume fraction to saturate at 10 percent after

about 4 hours of tempering. By contrast, the retained austenite content of the QT material increases very slowly with tempering times; less than 3 percent retained austenite is present after 16 hours tempering. No hexagonal ε-martensite was detected in the final structure after any of these heat treatments.

B. Tensile Properties as a Function of Heat Treatment.

The results of tensile tests on the 5Mn alloy at room temperature and at liquid nitrogen temperature (-196°C) are presented in Table III. Both of the cyclic heat treatments (QQ'T and 2BT) lead to a slight decrease in room temperature yield strength relative to that of the QT material. The tensile strength, on the other hand, is relatively unaffected by heat treatment. The uniform and total elongations are significantly increased by cyclic heat treatment. The decrease in yield strength after cyclic heat treatment may result from the introduction of the softer austenite phase, or may rather be due to gettering of interstitials by the austenite, since the QT material shows a yield phenomena which is absent in the material given cyclic heat treatments.

In parallel to the case of Fe-Ni cryogenic alloys, both the yield and tensile strengths of the 5Mn alloy increase substantially on cooling to -196°C but become almost insensitive to heat treatment. On the other hand, the ductility, as measured either by the uniform elongation or by the reduction in area, is enhanced by cyclic heat treatment. The ductility is the greatest in the case of the 2BT material. The uniform elongation of these alloys is in all cases greater at -196°C than it is at room temperature.

C. The Influence of Heat Treatment on Impact Toughness and Transition Temperature.

The Charpy impact energy of the 5Mn alloy is plotted as a function of temperature and heat treatment (tempering at 590°C for 16 hours) in Fig. 8. The estimated percentage of ductile fracture in the impact fracture surface is also plotted.

The 5Mn alloy has an encouragingly low ductile-brittle transition temperature, -110°C, even in QT condition. However, the impact energy of the QT material at liquid nitrogen temperature is very low. Changing to the QQ'T heat treatment suppresses the ductile-brittle transition by ~55°C, but the material again shows very low impact toughness in liquid nitrogen. A change to the 2BT treatment suppresses the ductile-brittle transition temperature to below liquid nitrogen temperature (-196°C) and results in an excellent cryogenic impact toughness (~140 ft-lb, ~190J). The fracture mode of the 2BT material is predominately ductile at -196°C but with a slight intrusion of brittle fracture over 25 percent of the impact fracture surface.

The scanning electron fractographs presented in Fig. 9 show the change in appearance of the brittle portion of the impact fracture surface at -196°C with heat treatment. The fracture surface of the QT material contains a mixture of transgranular cleavage and intergranular fracture. In the QQ'T and the 2BT materials, the brittle portion of the fracture surface is entirely quasi-cleavage. Comparing the two cleavage fracture surfaces, the much smaller size of the cleavage facets in the 2BT material is apparent.

The observation of an intergranular fracture component in the QT material is not surprising since ferritic Fe-Mn steels are known to be susceptible to intergranular embrittlement[8-10]. The essentially complete elimination of intergranular fracture when the heat treatment is modified

to the QQ'T treatment is under continuing investigation but is believed to be associated with the precipitation and retention of austenite phase along the prior austenite grain boundaries. The relatively low ductile-brittle transition of the QQ'T material is believed to have two causes: the suppression of intergranular embrittlement, and the introduction of thermally stable retained austenite, which creates an effective refinement of the microstructure by impeding the cooperative cleavage of adjacent martensite laths[18]. The substantial further improvement in the ductile-brittle transition temperature when the heat treatment is modified to the 2BT treatment is presumably a consequence of the grain refinement achieved by the 2B thermal cycling which precedes the final temper. The symbiotic effect of grain refinement and retained austenite in suppressing the ductile-brittle transition temperature has been documented in the case of Fe-Ni alloys[14]. The present results would seem to show that similar benefits are obtainable in Fe-Mn alloys of relatively low manganese content.

The dependence of the fracture-appearance transition temperature (FATT corresponding to ~50% visually brittle fracture on the impact specimen surface.) on the tempering time and pretempering heat treatment is presented in Fig. 10. The associated Vickers hardness of the alloys (at room temperature) is also plotted. As the tempering time is increased both the hardness and the FATT decrease, reaching nearly asymptotic values after 4 hours tempering in both the QQ'T and 2BT materials. On the basis of these data it does not appear that further increases in tempering time would be more than marginally beneficial to the QQ'T material. A grain refinement treatment, such as accomplished by the 2BT thermal cycling, seems essential to achieve adequate cryogenic toughness at -196°C in Fe-5MN alloys.

D. The Influence of Carbon Content.

The ingots labelled C, D, and E in Table I were cast to assess the effect of carbon content on the cryogenic properties of the 5Mn alloy. The high-carbon ingots were given the 2BT treatment indicated for the 5Mn alloy in Table II and their FATT and Charpy impact energies at -196°C were determined. The results are plotted in Fig. 11.

The results show that the properties of the 5Mn alloy deteriorate for carbon contents above 0.04 wt.% by an amount which increases either with carbon concentration or with tempering time. The metallurgical source of this deterioration has not yet been determined but the observation that the properties of the alloy are poorer after a 16-hour temper than after a 4-hour temper suggests that carbide precipitation plays a role. The data may also be read to infer that alloys having carbon contents less than 0.04 wt.% C would have still better properties. This possibility is under investigation, although preliminary experiments suggest that the alloys must contain at least some carbon if an optimal tempering response is to be obtained.

E. The Influence of Manganese.

The results obtained to date suggest that there is no significant change in alloy properties with the small (less than 1 wt.%) variations in manganese content which result from normal casting practice. However, the properties of the alloy do deteriorate significantly when the manganese content is increased to 8 wt.%.

Research on alloys containing 8 wt.% Mn was done, in part, to shed additional light on the observation by Hwang and Morris[11] that the 2BT treatment was not sufficient to impart good toughness in an Fe-8Mn-0.2Ti alloy at -196°C. The alloy studied in this research is that designated H in

Table I and had nominal composition Fe-8Mn-0.02Mo-0.06C. This alloy was given the 2BT heat treatment tabulated in Table II. The properties of this alloy after tempering for either one hour or 16 hours at 590°C are presented in Fig. 12.

It is apparent from the data presented in Fig. 12 that, in this case also, the utilization of the 2BT treatment is not sufficient to establish toughness in the 8Mn alloy at -196°C. At least part of the poor toughness response of the 8Mn composition is attributable to its higher yield strength and its higher carbon content relative to the best 5Mn composition. It is, however, interesting to note a contrast in the response of the FATT to tempering time between the 5 and 8Mn compositions. In the 5Mn alloy the FATT decreases dramatically as the tempering time is raised from 1 to 16 hours. This decrease is associated with a significant increase in the volume fraction of retained austenite, from ~3% to ~10%. No ε-martensite is detected in the 5Mn alloy after higher heat treatment. In the case of the 8Mn alloy, by contrast, there is virtually no change in the FATT with increasing tempering time even though the yield strength of the alloy drops substantially. There is also virtually no change in the retained austenite content of the 8Mn alloy (~15%) as the tempering time is increased, but there is a substantial increase in the volume fraction of ε-martensite, from ~0% to ~30%. Hwang and Morris[11] have previously pointed out that the low-temperature toughness of Fe-Mn ferrites is sensitive to the retained austenite content but appears to be relatively insensitive to the presence of ε-martensite. This conclusion is supported by the results of the present research.

It would appear from this result that the successful toughening of higher manganese ferritic steels for cryogenic use will require the use of a grain refining treatment such as the 2B treatment supplemented by

alloy modifications to promote the formation of thermally stable austenite while suppressing the appearance of the ε-martensite phase.

F. The Effect of Nickel Additions.

The addition of a small amount of Ni to the 5Mn base composition was found to be decidedly beneficial. Ingots F and G in Table I were cast to study the nickel effect. These alloys contained nominal additions of 1 and 3 wt.% Ni to the base 5Mn alloy. They were tested in the 2BT condition using the heat treatment temperatures tabulated in Table II.

The tensile properties of the nickel-modified alloys were determined at room and liquid nitrogen temperatures and are presented in Table III. The yield strength increases significantly with Ni content; the 5Mn-3Ni alloy has a yield strength exceeding that of commercial 9Ni steel.

The room temperature tensile properties, the Charpy impact energy at -196°C, and the volume fraction of retained austenite is plotted as a function of Ni content and tempering time in Fig. 13. Despite the increase in yield strength, the Charpy impact energy at liquid nitrogen temperature remains high, a result which seems attributable, at least in part, to the increasing retention of austenite as the Ni content is raised. The estimated fraction of brittle fracture on the surface of Charpy specimens broken in liquid nitrogen decreases slightly as the Ni content is raised from approximately 25% brittle fracture at 0% Ni to approximately 15% at 3% Ni.

G. Cryogenic Fracture Toughness.

The results of fracture toughness tests on both the 2BT-treated 5Mn steel and the Ni-modified 5Mn steels at -196°C are presented in Table IV. Plane-strain conditions were not established in any of these tests. Plane-strain fracture toughness (K_{1c}) values were hence estimated using equivalent

energy[22] K_{1c}^{E} and J-integral[23] K_{1c}^{J} methods. A reference value of the critical flaw size for fracture was also calculated from the square of the ratio of the estimated K_{1c} to the yield strength.

The estimated fracture toughness of 5Mn steel at -196°C is near 100 Ksi $\sqrt{in.}$ (110 MPa $\sqrt{m}$), which further documents the excellent toughness of the alloy. The fracture toughness increases with Ni content. The estimated critical flaw size, $(K_{1c}/\sigma_y)^2$, lies between 0.5 and 0.8 inches (13 and 19mm) for all three 5Mn based steels.

IV. CONCLUSIONS

By way of summary, the strength-toughness characteristics of the 2BT-treated 5Mn and Ni-modified 5Mn alloys are plotted in Fig. 14 in comparison with those of 9Ni steel in the QT and NNT conditions[14,15], 304 stainless steel[14], and boron-modified 12Mn[19]. As will be seen from the figure, the strength-impact toughness combinations of these low-alloy cryogenic steels are competitive with that of 9Ni steel at liquid nitrogen temperature and are decidedly superior to that of the 304 stainless steel. The fracture toughnesses of the 5Mn alloys are somewhat inferior to those of 9Ni and 304 stainless steel, but are nonetheless good, and may prove satisfactory for a variety of low-temperature structural applications.

ACKNOWLDGMENTS

This work was supported by the Division of Materials Sciences, Office Basic Energy Sciences, U. S. Department of Energy, under contract No. W-7405-Eng-48.

REFERENCES

1. D. A. Sarno and J. B. Bruner: Advances in Cryogenic Engineering, 1978, vol. 24, p. 529.
2. S. Nagashima, T. Ooka, S. Sekino, H. Mimura, T. Fujishima, S. Yano, and H. Sakurai: Trans. Iron Steel Inst. Jpn., 1971, vol. 11, p. 402.
3. J. W. Morris, Jr., S. K. Hwang, K. A. Yushchenko, V. I. Belotzerkovetz, and O. G. Kvasnevskii: Advances in Cryogenic Engineering, 1978, vol. 24, p. 91.
4. M. J. Schanfein, M. J. Yokota, V. F. Zackay, E. R. Parker, and J. W. Morris, Jr.: Properties of Materials for Liquified Natural Gas Tankage, ASTM STP 579, p. 361, 1975.
5. H. Yoshimura, N. Yamada, and H. Yada: Trans. Iron Steel Inst. Jpn., 1976, vol. 16, p. 98.
6. K. A. Yushchenko: Advances in Cryogenic Engineering, 1978, vol. 24, p. 120.
7. T. Kato, S. Fukui, M. Fujikura, and K. Ishida: Trans. Iron Steel Inst. Jpn. 1976, vol. 16, p. 673.
8. M. J. Roberts: Met. Trans., 1970, vol. 1, p. 3287.
9. A. Holden, J. D. Bolton, and E. R. Petty: J. Iron Steel Inst., 1971, vol. 209, p. 721.
10. J. D. Bolton, E. R. Petty, and G. B. Allen: Met. Trans., 1971, vol. 2, p. 2915.
11. S. K. Hwang and J. W. Morris, Jr.: Met. Trans. A, 1979, vol. 10A, p. 545.
12. J. W. Morris, Jr., S. Jin, and C. K. Syn: Trans. Jpn. Int. Metals, 1976, vol. 17 (Suppl.), p. 393.
13. S. Jin, J. W. Morris, Jr., and V. F. Zackay: Met. Trans. A, 1975, vol. 6A, p. 141.

14. S. Jin, S. K. Hwang, and J. W. Morris, Jr.: Met. Trans. A, 1975, vol. 6A p. 1721.

15. C. K. Syn, S. Jin, and J. W. Morris, Jr.: Met. Trans. A, 1976, vol. 7A, p. 1827.

16. C. W. Marshall, R. F. Heheman, and A. R. Troiano: Trans. ASM, 1962, vol. 55, p. 135.

17. S. Yano, H. Sakurai, H. Mimura, N. Wakita, T. Ozawa, and K. Aoki: Trans. Iron Steel Inst. Jpn., 1973, vol. 13, p. 133.

18. J. W. Morris, Jr., C. K. Syn, J. I. Kim, and B. Fultz: Proceedings, Int. Conf. on Martensitic Transformations (ICOMAT), Cambridge, Mass., June, 1979, in press.

19. S. K. Hwang and J. W. Morris, Jr.: Met. Trans., in press. 1980.

20. M. Niikura, M. Yamada, J. Tanaka, and H. Ichinose: Trans. Jpn. Inst. Metals, 1976, vol. 17 (suppl.), p. 321.

21. R. L. Miller: Manganese, special issue of Materiaux et Techniques, 1977, Dec., p. 55.

22. F. J. Witt and T. R. Mager: Nucl. Eng. Des., 1971, vol. 17, p. 91.

23. J. A. Begley and J. D. Landes: ASTM STP 536, p. 246, Amer Soc. Test. Mater., 1973.

24. J. W. Morris, Jr., C. K. Syn and J. I. Kim: Proceedings 25th Sagamore Army Materials Research Conference, Bolton Landing, N.Y., July, 1978.

TABLE I. Chemical Composition of Steels (wt-%).

Steel	Remarks	C	Mn	Mo	Ni
A	Base	0.038	4.40	0.20	
B		0.042	4.78	0.20	
C	High C	0.061	4.93	0.20	
D		0.081	4.69	0.20	
E		0.120	4.86	0.34	
F	High Ni	0.056	4.91	0.20	0.96
G		0.045	4.72	0.20	2.97
H	High Mn	0.065	7.98	0.20	

TABLE II. Heat Treatment Condition.

(°C)

	AN	1A	1B	2A	2B	T
5Mn	900	820	740	800	740	590
5Mn-1Ni	900	790	730	770	730	590
5Mn-3Ni	900	765	710	745	710	590
8Mn	900	740	650	720	680	590
	2 hrs AC	1 hr WQ	1 hr WQ	1 hr WQ	1 hr WQ	4-16 hrs WQ

TABLE III. Tensile Properties.

		YS Ksi (MPa)	TS Ksi (MPa)	Uniform Elong. %	Total Elong. %	RA %	Temp.
5Mn	QT	83 (573)	94 (649)	11.6	31.9	84.0	R.T.
		136 (938)	146 (1007)	18.7	34.1	65.9	-196°C
	QQ'T	69 (476)	92 (635)	19.2	40.6	85.0	R.T.
		133 (918)	147 (1014)	23.4	39.1	72.2	-196°C
	2BT*	72 (497)	97 (669)	19.6	41.3	85.7	R.T.
		138 (952)	152 (1049)	24.5	39.5	75.5	-196°C
5Mn-1Ni	2BT†	89 (614)	107 (738	18.9	36.8	84.3	R.T.
		147 (1014)	167 (1152)	25.2	44.4	77.3	-196°C
5Mn-3Ni	2BT†	105 (724)	119 (821)	12.0	29.1	83.2	R.T.
		160 (1104)	181 (1249)	25.2	39.9	76.4	-196°C
9Ni	QT	100 (690)	110 (759)	-	25.0	66.0	R.T.
		146 (1007)	172 (1187)	-	30.0	66.8	-196°C
	NNT	90 (621)	110 (759)	-	20.0	63.0	R.T.
		145 (1000)	163 (1125)	-	34.0	72.0	-196°C

* 590°C x 16 hrs

† 590°C x 4 hrs

TABLE IV. Fracture Toughness Testing Results (2BT Treated 5Mn Steel).

	CHARPY	COMPACT TENSION				3-POINT BENDING	
	Cv ft-lb (Joules)	K_Q Ksi $\sqrt{in}$ (MPa $\sqrt{m}$)	K^E_{1c} Ksi $\sqrt{in}$ (MPa $\sqrt{m}$)	K^J_{1c} Ksi $\sqrt{in}$ (MPa $\sqrt{m}$)	$a=(\frac{K^J_{1c}}{\sigma})^2$ in (mm)	K Ksi $\sqrt{in}$ (MPa $\sqrt{m}$)	COD mil (mm)
5Mn	141 (191)	98 (108)	98 (108)	102 (112)	0.55 (14)	97 (107)	4.48 (0.114)
5Mn-1Ni	100 (136)	112 (124)	112 (123)	123 (123)	0.7 (18)		
5Mn-3Ni	108 (146)	105 (116)	124 (136)	140 (154)	0.76 (19)	109 (120)	4.12 (0.105)
9Ni(NNT)	125 (169)	157 (173)	210 (231)	197 (217)	1.85 (47.0)		
9Ni(QT)	92 (125)	140 (154)	168 (185)		1.46* (37.1)		

Testing Temperature: -196°C

Compact Tension: 0.7 in. Thickness : Thickness Requirement is not met for all steels.

3-Point Bending: 10mm x 10mm x 55mm with fatigued notch of 5mm.

* Computed from K^E_{1c}

FIGURE CAPTIONS

1. Comparison of the Fe-rich section of the equilibrium phase diagrams and typical kinetic diagrams on water quenching for the Fe-Ni and Fe-Mn binary systems, showing the intrusion of the ε-martensite phase in the Fe-Mn system.
2. Comparison of the microstructure and brittle fracture modes in Fe-8Mn and Fe-12Mn alloys: (a) dislocated lath martensite structure of quenched Fe-8Mn; (b) blocky martensite structure of Fe-12Mn; (c) transgranular cleavage in Fe-8Mn broken by impact at -196°C; (d) intergranular failure in Fe-12Mn broken at -196°C.
3. Schematic drawing of the 2BT heat treatment as used in the processing of the Fe-5Mn alloys.
4. Optical micrographs showing the structure of the Fe-5Mn alloy after the QT, QQ'T, and 2BT treatments described in the text.
5. Transmission electron micrographs showing the change in the substructure of Fe-5Mn with tempering time in the 2BT treatment: (a) after 1 hr tempering; (b) after 4 hrs tempering.
6. Transmission electron microscopic analysis showing the retention of austenite in Fe-5Mn in the 2BT treatment.
7. The volume fraction of retained austenite in Fe-5Mn as a function of heat treatment and tempering time at 590°C.
8. The Charpy impact energy and percentage ductile fracture in Fe-5Mn as a function of heat treatment and temperature.
9. Scanning electron fractographs of brittle fracture in the impact fracture surface of Fe-(3-5)Mn at -196°C in the QT, QQ'T, and 2BT heat treatments.
10. Plot of the fracture appearance transition temperature and the Vickers hardness (at room temperature) for Fe-5Mn as a function of heat treatment and tempering time at -196°C.

11. The Charpy impact energy at -196°C and the fracture appearance transition temperature of Fe-5Mn as a function of carbon content and tempering time in the 2BT treatment.
12. Comparison of γ- and ε-content, room temperature tensile properties, and fracture appearance transition temperature for the 5Mn and 8Mn alloys in the 2BT condition for two tempering times.
13. Plot showing the retained austenite content, room temperature tensile properties, and Charpy impact energy at -196°C as a function of nickel addition to Fe-5Mn in the 2BT treatment.
14. Comparative plot of Charpy impact energy and estimated fracture toughness against yield strength (all at -196°C) for the Fe-5Mn alloys discussed here, 9Ni steel in the QT and NNT conditions[14,15], 304 stainless steel[14], and the boron-modified Fe-12Mn alloy described in ref. 19.

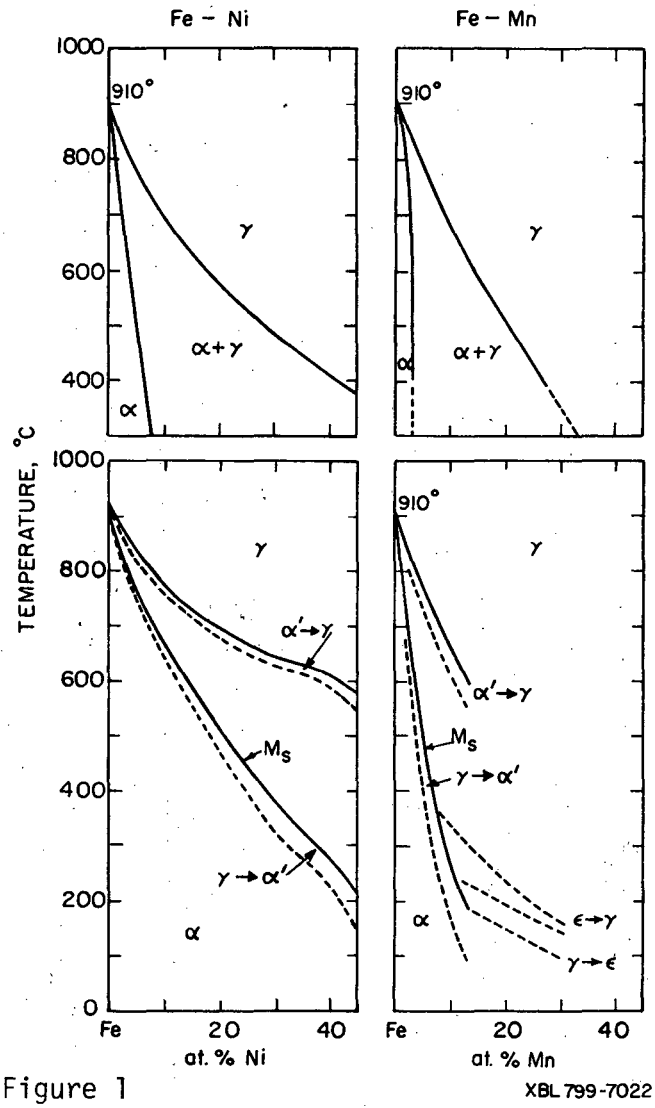
Fe – Ni
Fe – Mn
TEMPERATURE, °C
1000
800
600
400
200
0
910°
γ
α+γ
α
α'→γ
Ms
γ→α'
ε→γ
γ→ε
Fe
20
40
at. % Ni
at. % Mn
XBL 799-7022

Figure 1

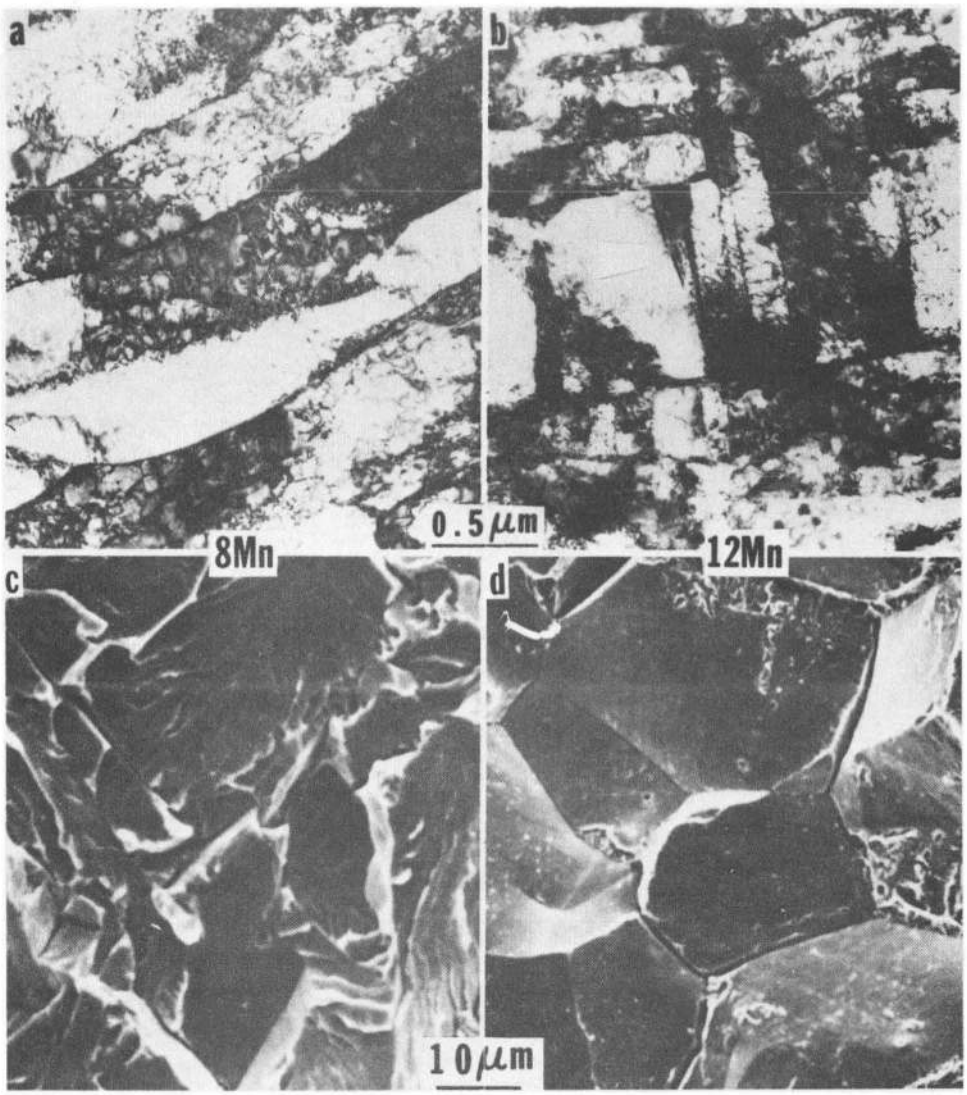

Figure 2

XBB 799-11380

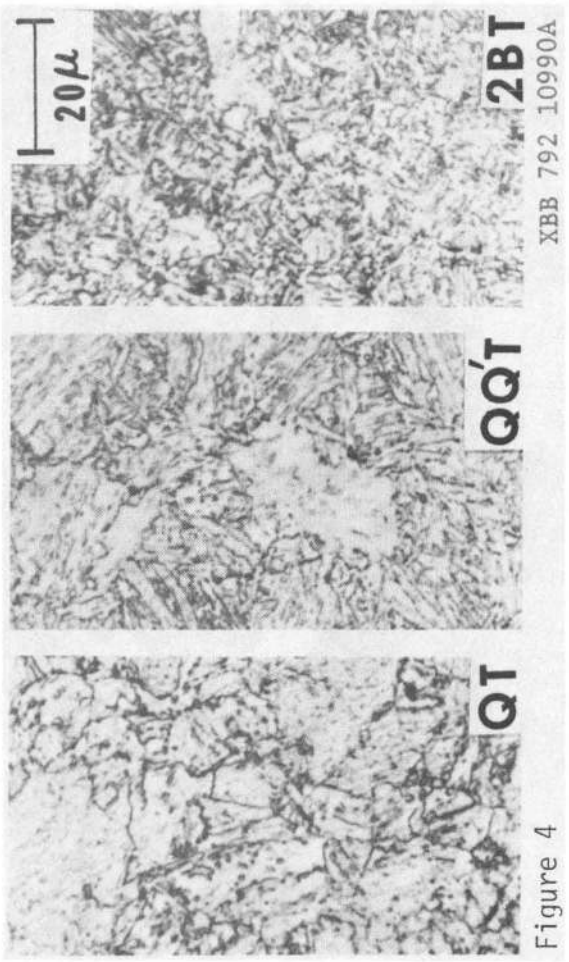

Figure 4

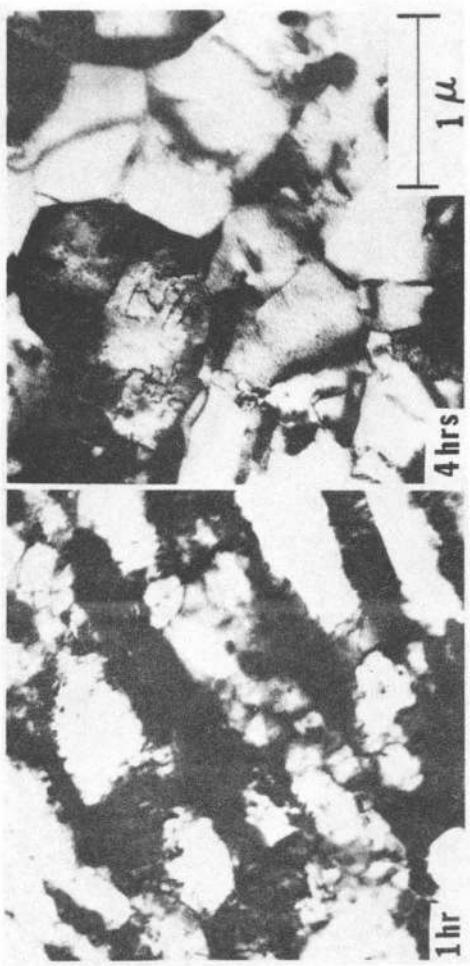

XBB 799-11379

Figure 5

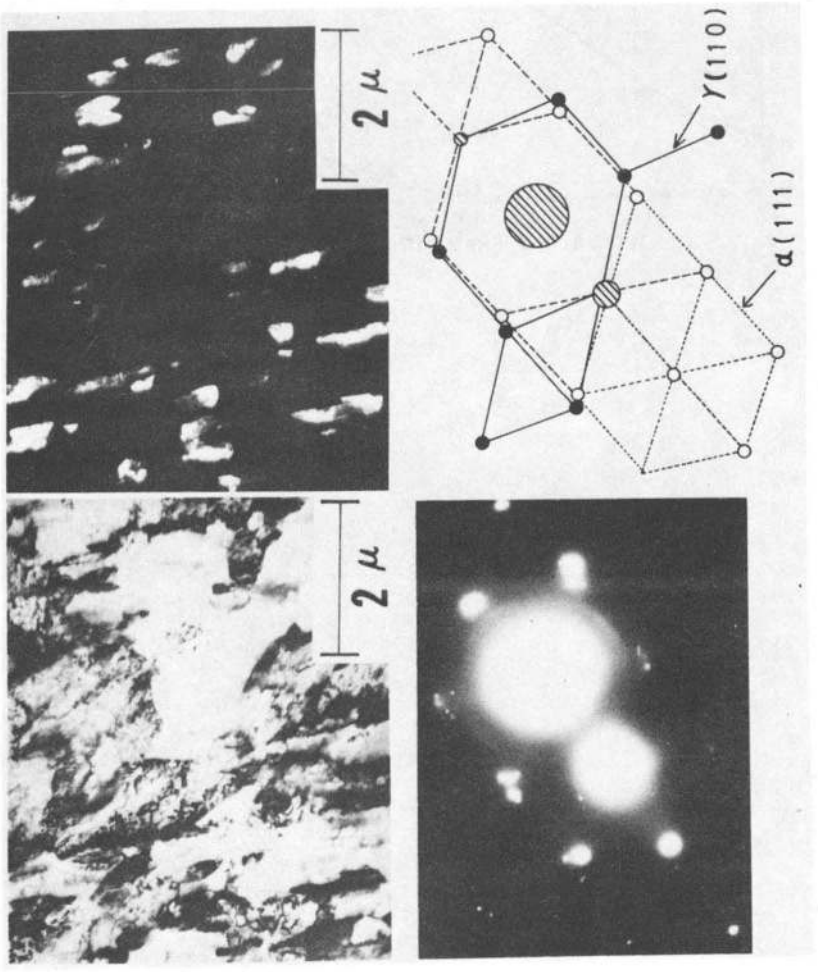

XBB 792-1994

Figure 6

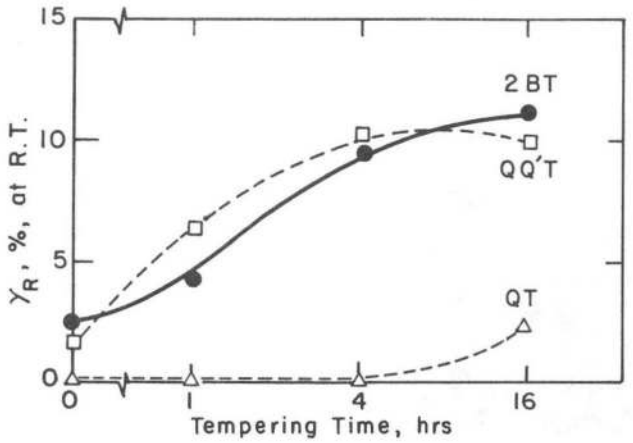

Figure 7

XBL798-6767

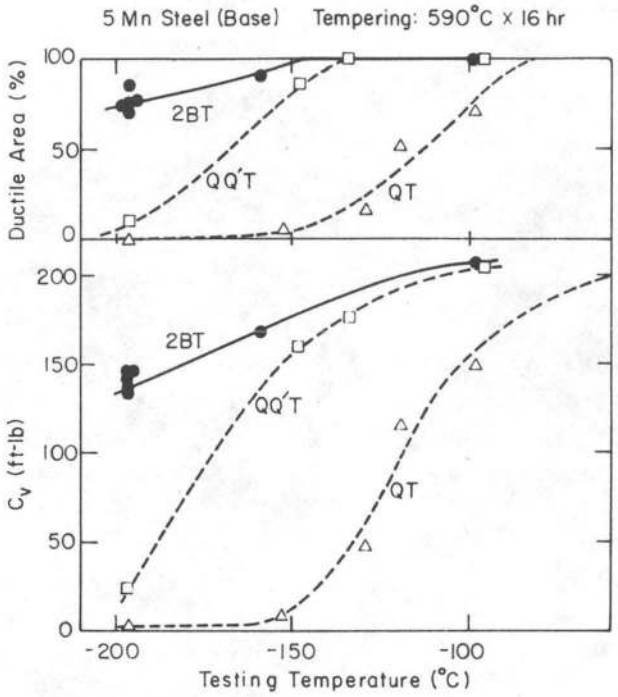

Figure 8

XBL792-5701

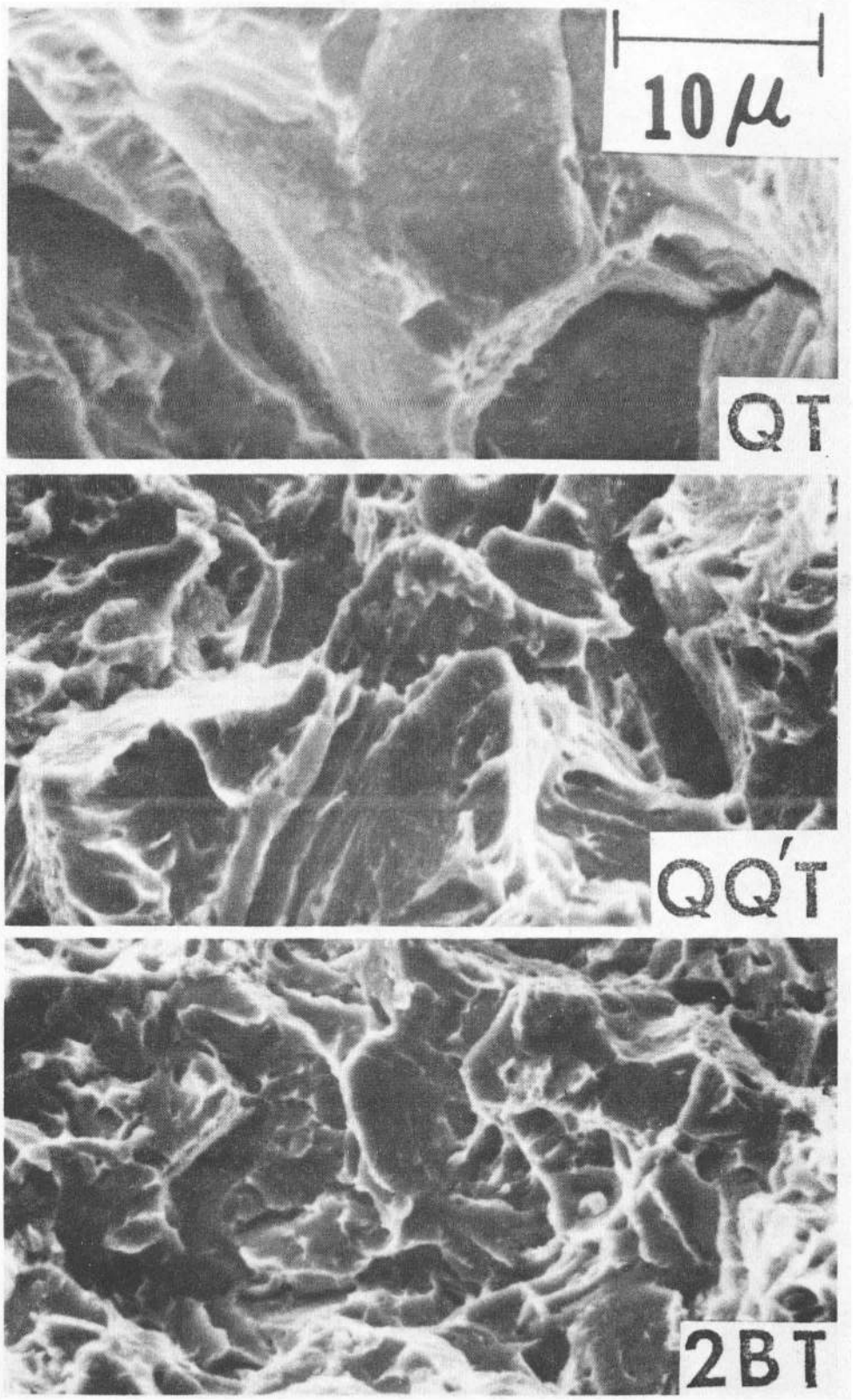

Figure 9

XBB 792-1991A

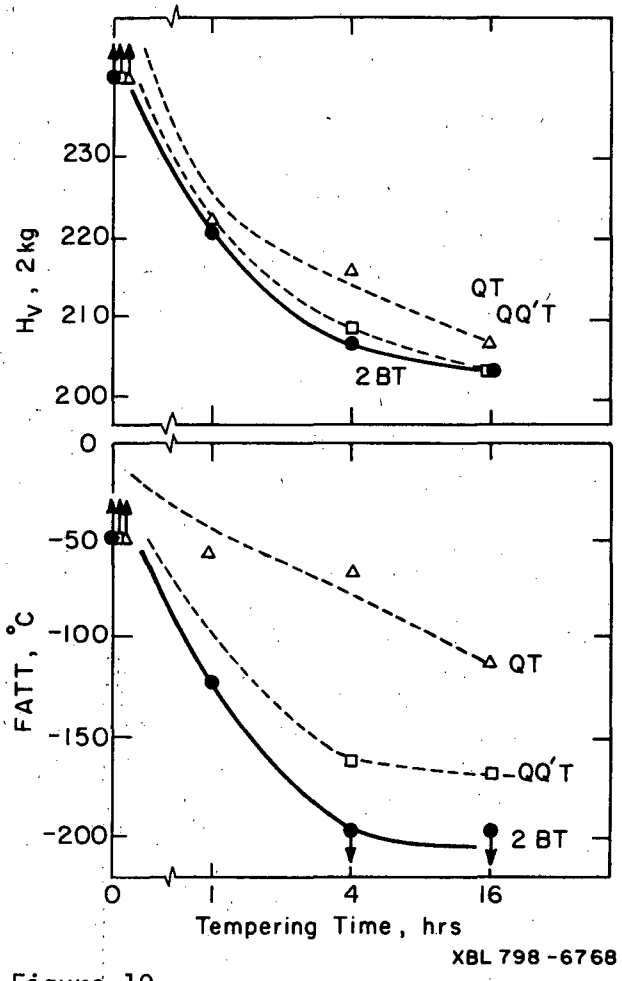
230
220
210
200
H_V, 2kg
QT
QQ'T
2BT
0
-50
-100
-150
-200
FATT, °C
QT
QQ'T
2 BT
0
1
4
16
Tempering Time, hrs
XBL 798-6768

Figure 10

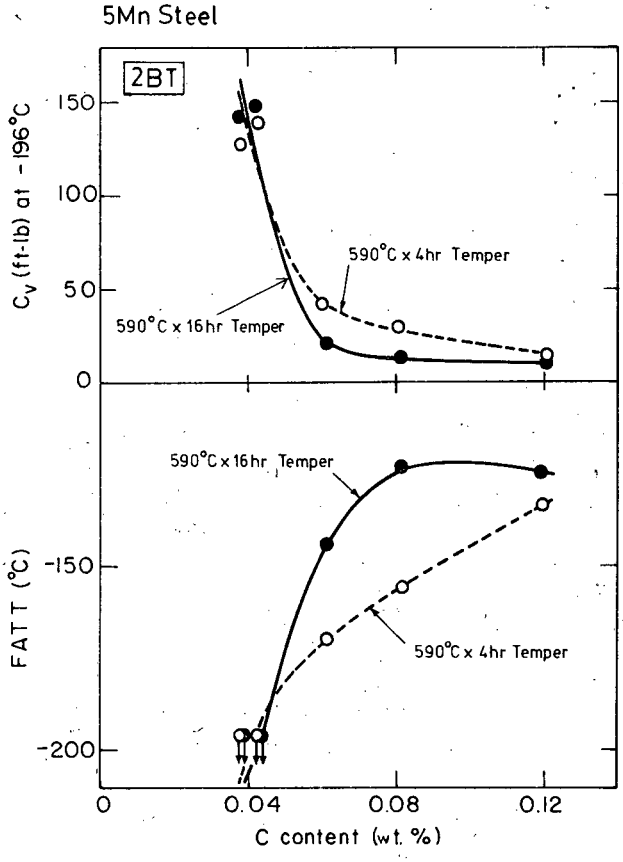
5Mn Steel
2BT
150
100
50
0
C_v (ft-lb) at -196°C
590°C x 4hr Temper
590°C x 16hr Temper
590°C x 16hr Temper
590°C x 4hr Temper
-150
-200
FATT (°C)
0
0.04
0.08
0.12
C content (wt. %)
XBL792-5699

Figure 11

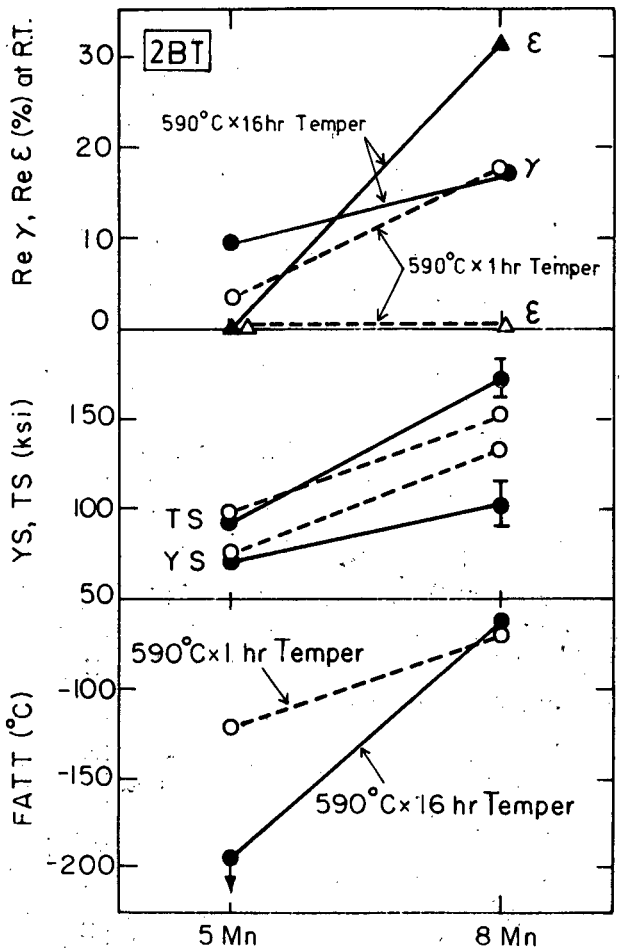

Figure 12

XBL792-5697

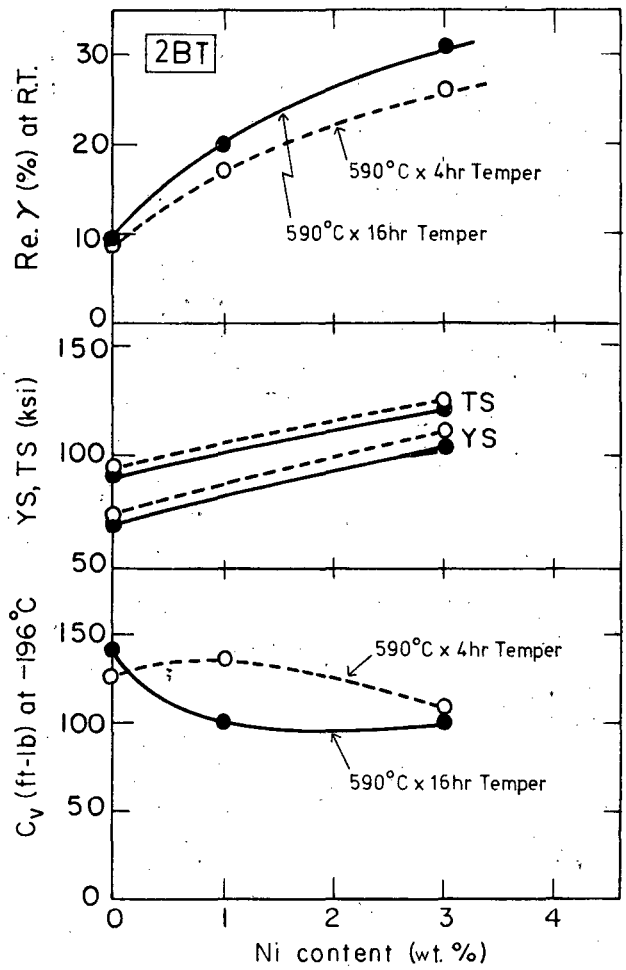

Figure 13

XBL 792-5698

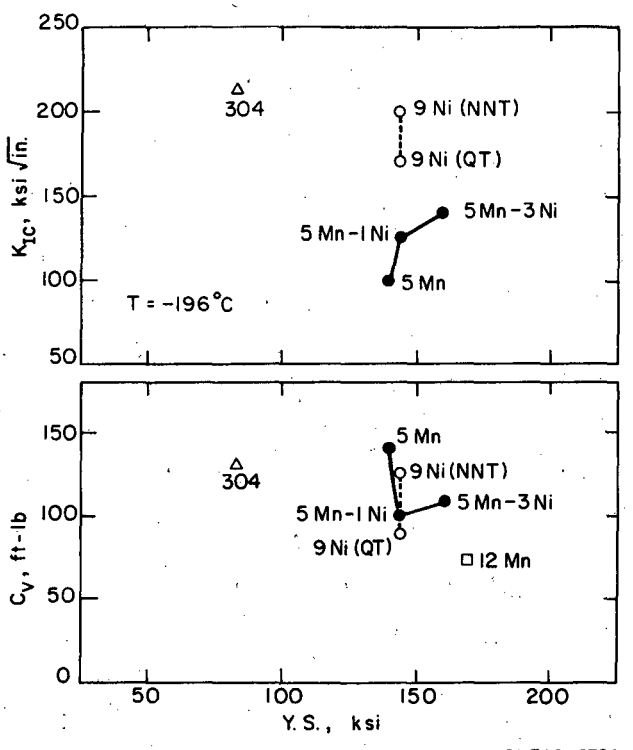
250
200
150
100
50
K_{Ic}, ksi $\sqrt{in.}$
304
9 Ni (NNT)
9 Ni (QT)
5 Mn-3 Ni
5 Mn-1 Ni
5 Mn
T = -196°C
150
100
50
0
C_V, ft-lb
304
5 Mn
9 Ni (NNT)
5 Mn-3 Ni
5 Mn-1 Ni
9 Ni (QT)
12 Mn
50
100
150
200
Y.S., ksi
XBL798-6766

Figure 14

TECHNICAL INFORMATION DEPARTMENT
LAWRENCE BERKELEY LABORATORY
UNIVERSITY OF CALIFORNIA
BERKELEY, CALIFORNIA 94720